

ANALYSIS OF THE LEVITATION CHARACTERISTICS OF SUPERCONDUCTING MAGNETIC BEARINGS

H. Fukuyama,^{1,*} T. Takizawa¹

ABSTRACT

A new calculation method for the levitation characteristics of superconducting magnetic bearings (SMBs) is presented. The method is based both on electromagnetic FEM of the magnetic field and the 2 dimensional Bean Model for analysis of magnetization of type II superconductors. To obtain magnetizing hysteresis, a superconductor is meshed into cells for calculation. The patterns of the hysteresis are grouped into 31 cases according to variation of the parameters which are the length of the a and b sides of the cell, critical current density J_c , amplitude of the varying magnetic field ΔH and the field cooling magnetic field strength H_0 . Computer subroutines were made for all 31 cases in order to calculate levitation force hysteresis of any kind of SMBs in a short time. Close agreement was achieved between calculation and experiment on levitation characteristics.

INTRODUCTION

YBaCuO superconductors fabricated by the so called melt-grown process (QMG)[1] or melt-powder-melt-growth(MPMG)[2] shows very strong magnetic force. Many experimental investigations have been reported on Superconducting magnetic bearings (SMBs) of the combination of these superconductors and magnets[3-6]. Recently SMBs have been researched for applying to energy storage flywheel systems due to their low frictional characteristics[7-10]. In the design of flywheel system, it is important to evaluate correct levitation force of SMBs. Several researches have been reported about the numerical analysis of magnetic force between a high- T_c superconductor and a permanent magnet. Chang [11] calculated magnetic force acting on a ceramics superconductor by using magnetization curve. Sugiura [12] applied the magnetic vector potential (A) method to solve the Maxwell equations with a nonlinear J-E relation based on the critical state model [13]. Hashizume [14] applied the current vector potential (T) method to the finite element analysis of the AC losses of a type II superconductor in a two-dimensional geometry. Uesaka [15] developed a three-dimensional computing method for levitation analysis based on current vector potential (T) method. Tsuchimoto [16] analyzed numerically vertical levitation force in axisymmetric model using magnetic vector potential(A), and horizontal restoring force using current vector potential (T) method.

For the purpose of sufficient energy storage, the weight of flywheels should be very large. SMBs applied to energy storage flywheel systems are large in size, so it is impossible to make the superconductors with a single crystal. The superconductors should have a polycrystal structure or be assembled with a number of single crystal bulk superconductors. Furthermore, the magnetic field acting on superconductors is not uniform but complex. In our new calculation

*Tel: +81-466-21-3230; fax: +81-466-27-9766; e-mail: fukuyama-hiromasa@ov.nsk.com.

¹NSK Ltd. 1-5-50, Kugenuma Shinmei, Fujisawa-shi Kanagawa, Japan.

method, the effect of this complex magnetic field on the magnetization of each single crystal composing a polycrystal can be correctly reflected. The objectives of this paper are to present this new calculation method for the levitation characteristics of these complex SMB structures, to show good agreement of calculation results with experimental results and to show analytical results of the effects of parameters.

ANALYSIS MODEL

Fig 1 illustrates a scheme of our analysis. In this figure, there are two magnet rings, but this is not restricted, there may be three or four or so on. The superconductor ring is composed of numerous single crystal bulk superconductors, and they are adhered to each other as shown (1). The magnets move up and down. The superconductor ring is meshed into cells in the analysis. The magnetic field created by the magnetic rings is calculated with the finite element method (FEM) assuming that the superconductor is only vacuum space. (2) and (3) show the magnetic field and the magnetic flux acting on the meshed cells.

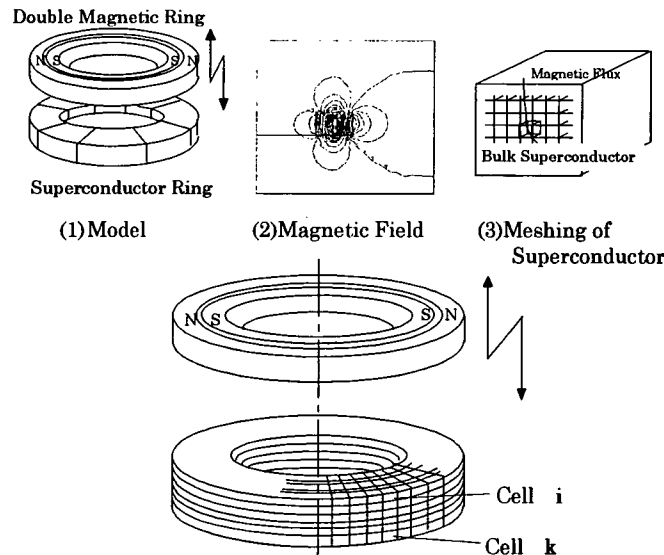


Figure 1. Model of analysis

MAGNETIZATION ANALYSIS

The analysis of magnetization generated in a superconductor is done by applying the 2 dimensional Bean critical state model to meshed cells. Fig.2 shows schematic illustrations of the magnetization process in a meshed cell according to the change of acting magnetic field. In this figure, a meshed cell, solid state illustrations of the magnetization and orthographies of a-h plane and b-h plane of the magnetization are illustrated. Here a and b are the a side and b side of the meshed cell, and c is the height of the cell. H_{act} is the acting external magnetic field. H_0 is the field cooling magnetic field. H_U is the highest acting magnetic field that corresponds to the nearest approach of the magnet rings to the superconductor. H_L is the lowest magnetic field that corresponds to the farthest the magnets get from the superconductor. The state (1) to (2) is the increasing external field. In this step, repulsive magnetization increases with increases in the external field. Magnetization is represented as the volume of the solid which is enclosed within the lines whose gradients are $\text{rot } \mathbf{B} = \mu_0 \mathbf{j}_c$. The state (2) is the nearest approach of the magnets to the superconductor. The process from (2) to (4) is the decreasing external field

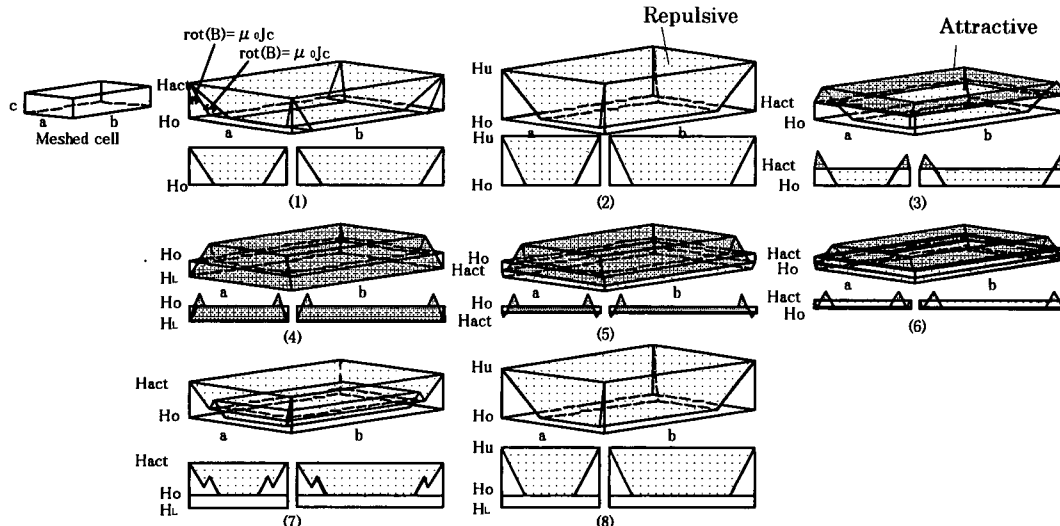


Figure 2. Magnetization hysteresis by the 2 dimensional Bean model

case. In this step, attractive magnetization is generated and increases canceling the previous repulsive magnetization. The state (4) is the farthest the magnetic rings get from the superconductor and the magnetization becomes only attractive. In (4) to (8), the increasing external field corresponds to the approach of the magnets to the superconductor. The state (8) is the same as (2). After (8), the process from (2) to (8) is repeated. Thus, repulsive and attractive magnetization is generated as hysteresis phenomena when magnets approach and remove from a superconductor.

When we calculate the magnetization of each meshed cell, we must consider the effect of meshing. This effect is illustrated by Fig.3 which shows the magnetization of a single crystal by the 1 dimensional Bean model. The crystal is large enough for the acting magnetic field to not be uniform as shown by broad line in Fig.3. In Fig.3, the crystal is divided into 4 parts and in each part the average acting magnetic field ($H_{a1}, H_{a2}, H_{a3}, H_{a4}$) is different from each other. In the figure, the whole average acting magnetic field of the entire crystal is also represented as H_a . Magnetization calculated in the divided parts by Bean model is represented by hatched triangle. This magnetization is not correct. It should be corrected as follows.

Accurate magnetization generated in part ① where average magnetic field H_{a1} is acting can be obtained by widening that part size ($W/4$) to whole size (W), acting H_{a1} on the whole size and dividing the obtained magnetization by 4. The same procedure is used in the other parts. Magnetization of the divided parts by this means is shown in Fig.3. The total magnetization of the whole crystal should be the sum of the magnetization of the 4 parts.

In the 2 dimensional Bean model, the same procedure is used both in length and in width.

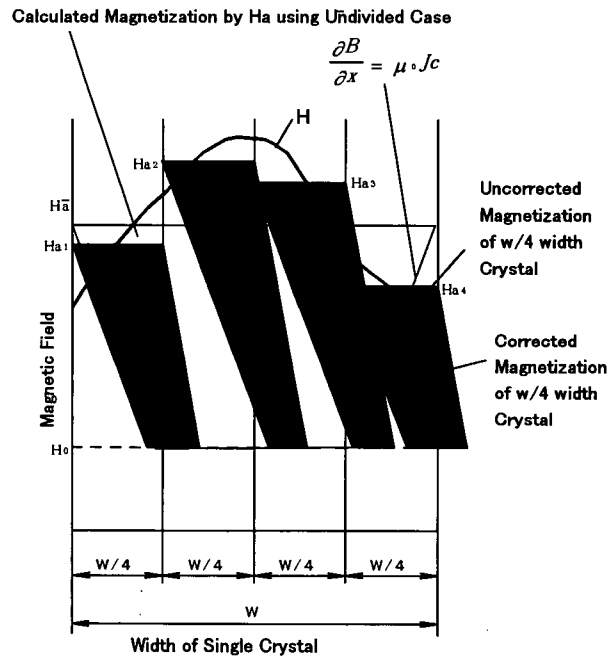


Figure 3. Correction of the effect of meshing on magnetization

That is as follows. When a superconductor ring is meshed into cells, a single crystal is meshed by m in length and meshed by n in width as one group. In the calculation of the magnetization of the meshed cell, the length of the meshed cell is multiplied by m and the width is multiplied by n . The calculated magnetization is divided by $(m \times n)$ and then it becomes real magnetization of the meshed cell.

In the calculation of the magnetization hysteresis of a meshed cell by the 2 dimensional Bean model, patterns of magnetization hysteresis are grouped into a particular number of cases according to 5 parameters which are a , b , J_c , ΔH and H_0 . And the acquired number of subroutines for calculation of magnetization are formed. Then the magnetization hysteresis of the meshed cell can be calculated by calling from the subroutine group according to the parameters. Generally each meshed cell has particular and different a , b , ΔH , H_0 and J_c . The particular number is 31 with the restriction that $2a > b > a$. Fig.4 shows these 31 cases. For an example, in Fig.3, cell i and cell k have different ΔH and H_0 .

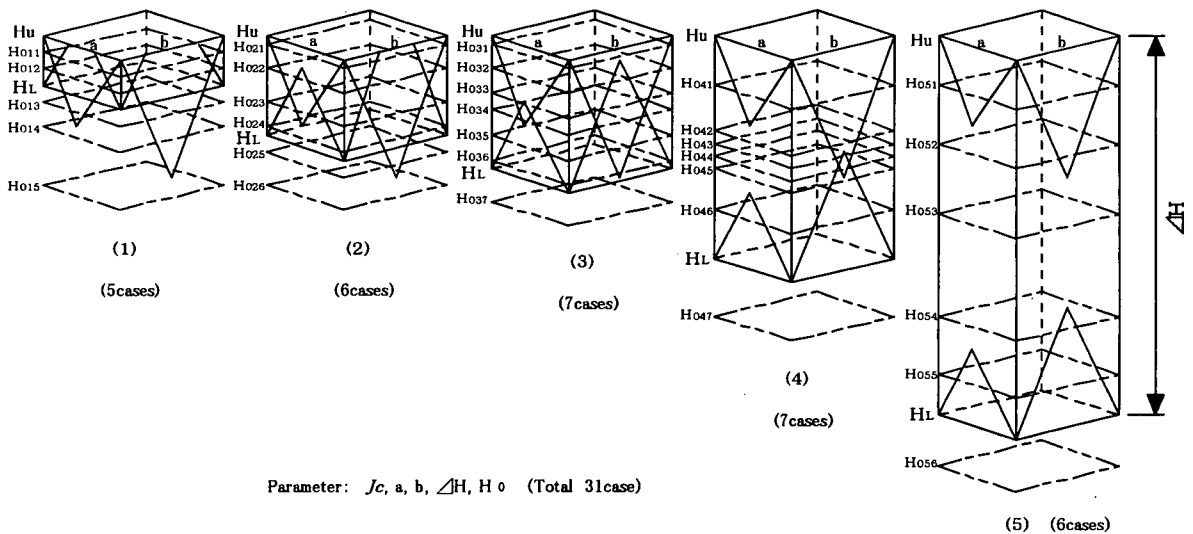


Figure 4. 31 Cases of magnetization hysteresis

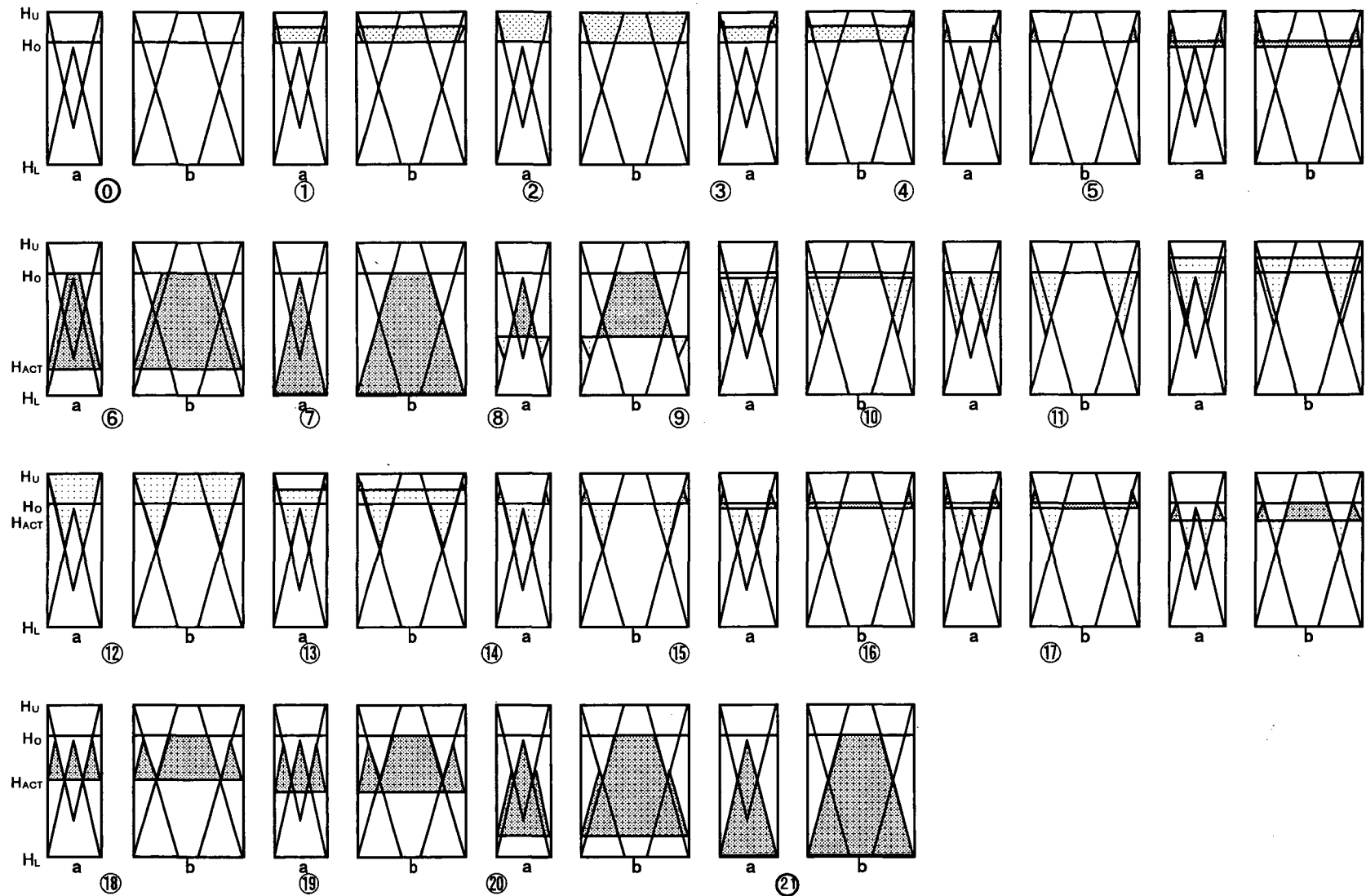
In Fig.4, (1) is the case in which the amplitude of the changing magnetic field $\Delta H (=H_U - H_L)$ is small enough compared to the critical current density J_c and the gradient line of repulsive magnetization (i.e. repulsive gradient) does not intersect with the gradient line of attractive magnetization (i.e. attractive gradient) in both the a - h plane and the b - h plane. The initial field cooling magnetic field H_0 may be $H_{011} \sim H_{015}$. H_{011} is the case in which the distance between the superconductor and magnets is very short in field cooling. On the other hand, H_{015} is the case in which the superconductor and the magnets are far apart in field cooling.

(2) is the case in which ΔH becomes larger in relation to J_c compared to (1) and in the a - h plane the triangle formed by the gradient lines of repulsive magnetization (i.e. repulsive triangles) intersects the triangle formed by attractive magnetization (i.e. attractive triangle) and in the b - h plane the repulsive gradient intersects with the attractive gradient. As to H_0 , there are 6 cases, $H_{021} \sim H_{026}$.

(3) is the case in which ΔH becomes still larger in relation to J_c . In both the a - h plane and the b - h plane, the repulsive triangles intersect with the attractive triangles. As to H_0 , there are 7 cases, $H_{031} \sim H_{037}$.

(4) is the case in which ΔH becomes considerably large in relation to J_c and in the a - h plane the repulsive triangle is separated from the attractive triangle and in the b - h plane the intersection of the two remains. Regarding H_0 , there are 7 cases, $H_{041} \sim H_{047}$.

(5) is the case in which ΔH becomes large enough for the said triangles to be separate from each other in both the a - h plane and the b - h plane. Regarding H_0 , there are 6 cases, H_{051}

Figure 5. Magnetization Hysteresis of H_{021}

~H₀₅₆.

Among these cases, we examined the H₀₂₁ case for an example. Fig.5 shows the hysteresis of magnetization of H₀₂₁ as orthographies of a-h plane and b-h plane. In this hysteresis , subroutines which need to be made are 11 in total which correspond to 10 subroutines representing 10 characteristic states (i.e.①、③、⑤、⑥、⑧、⑩、⑬、⑮、⑰、⑱) and one subroutine describing the whole hysteresis process. In this way ,55 subroutines are needed to calculate the magnetization hysteresis of H₀₁₁~H₀₅₆.

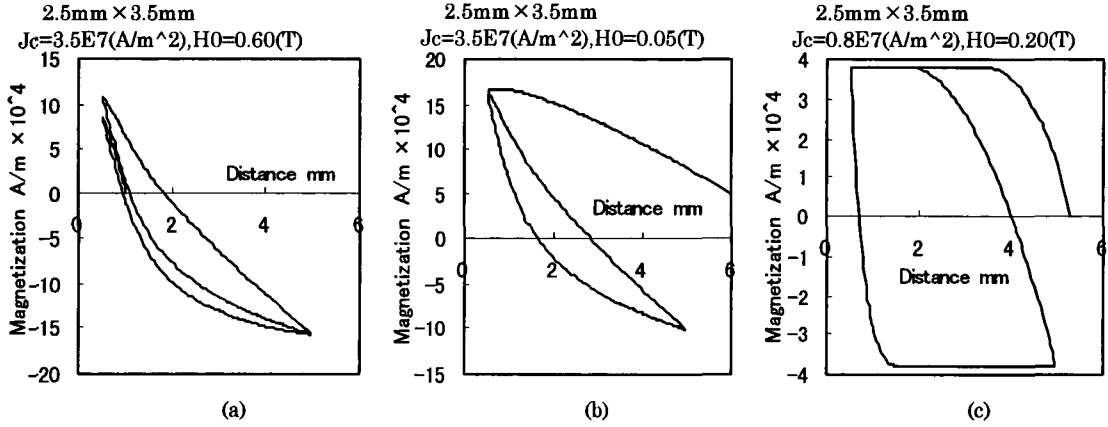


Figure 6. Calculation results of magnetization

Fig.6 shows 3 calculation results of 3 samples of magnetization hysteresis.

- (a) is an example of H₀₂₁.
- (b) is an example of H₀₂₆.
- (c) is an example of H₀₅₆.

LEVITATION FORCE ANALYSIS

The levitation force hysteresis of meshed cells can be obtained by calculating the hysteresis of the x, y, and z components of the levitation force of cells.

The levitation force f of a cell whose volume is dv can be calculated as follow

$$f = m \bullet \nabla B dv \tag{1}$$

here, m is magnetization, and B is magnetic flux density.

The levitation force F of the whole superconductor is

$$F = \int m \bullet \nabla B dv \tag{2}$$

Equation (2) is represented as follows.

$$\begin{aligned} F_x &= \sum \left(m_x \frac{\partial B_x}{\partial x} + m_y \frac{\partial B_x}{\partial y} + m_z \frac{\partial B_x}{\partial z} \right) dv \\ F_y &= \sum \left(m_x \frac{\partial B_y}{\partial x} + m_y \frac{\partial B_y}{\partial y} + m_z \frac{\partial B_y}{\partial z} \right) dv \\ F_z &= \sum \left(m_x \frac{\partial B_z}{\partial x} + m_y \frac{\partial B_z}{\partial y} + m_z \frac{\partial B_z}{\partial z} \right) dv \end{aligned} \tag{3}$$

m shows hysteretic phenomenon as said before according to change of magnetic position. The levitation force hysteresis is obtained by equation (1) using the hysteresis of m . The

levitation force hysteresis of the whole superconductor is obtained by equation (2) or (3). The calculated result of a similar case of parameter combination to Figure 5(a) was shown in Fig.6. Flow chart is expressed in Fig.7.

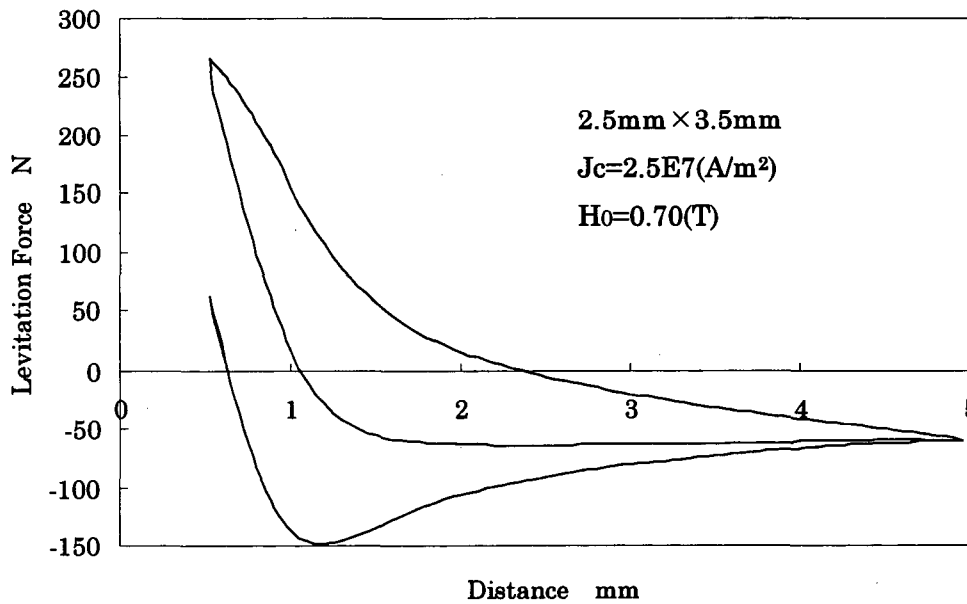


Figure 7. Levitation force hysteresis of the case of figure 5(a)

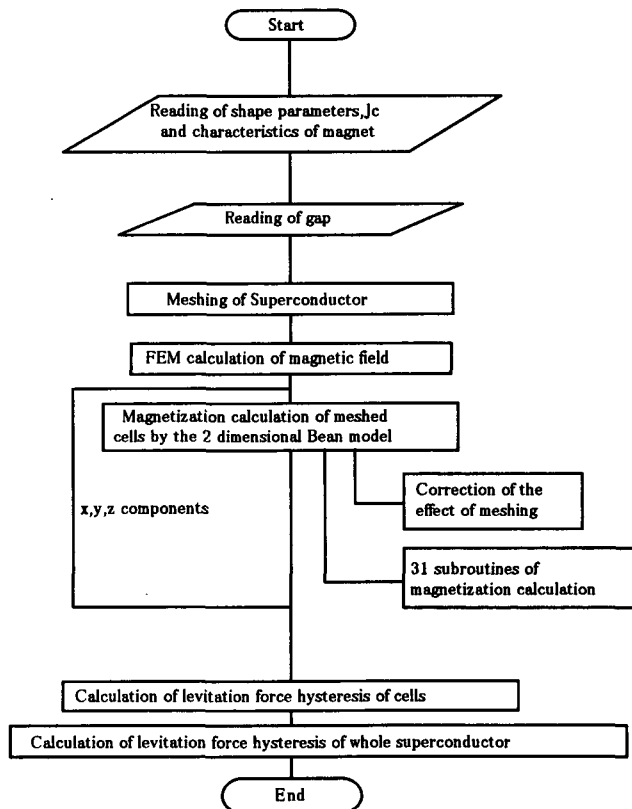


Figure 8. Flow chart

EXPERIMENT

The experimental equipment is shown in Fig.9. The configuration of the tested superconducting magnetic bearing is shown in Fig.10. Fig.11 and Fig.12 are the calculated B_z and B_x which are z and x components of magnetic flux density by FEM at various gaps. Fig.13 is the measured J_c of the tested superconductor. The superconductor ring was composed of 4 circular arc pieces and the ring size was $\phi 118 \times \phi 40 \times t15$. Each arc part was a single crystal of oxide high temperature superconductor of Y-Ba-Cu-O.

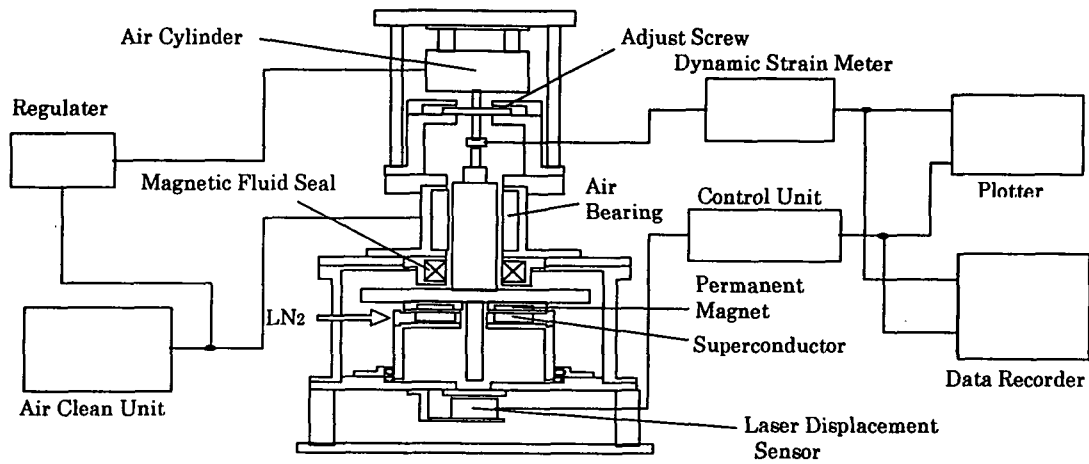
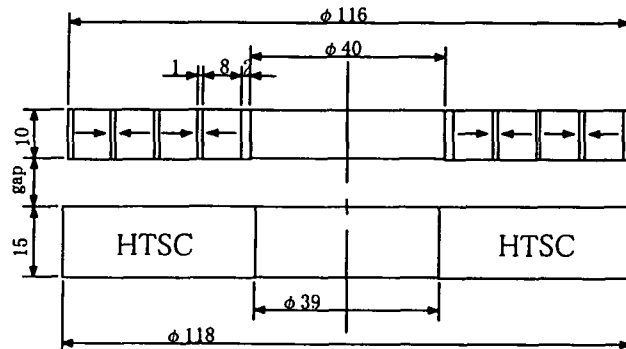
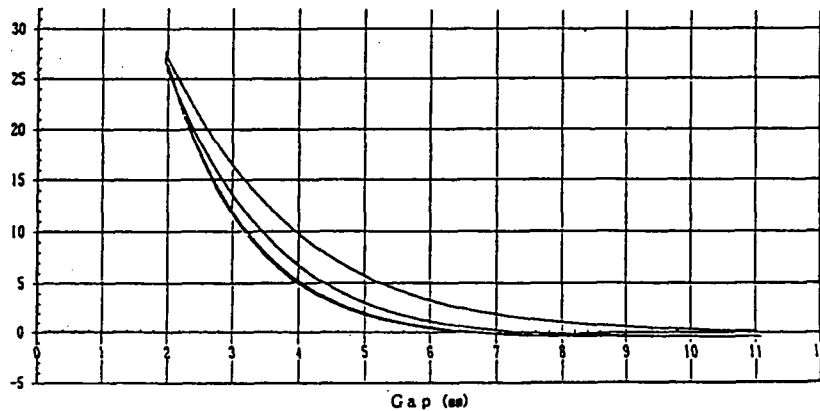


Figure 9. Experimental equipment



(a) Configuration of tested superconductor magnetic bearings



(b) Result of levitation test

Figure 10 Experimental object and tested result (Measured by Shikoku Research Institute Inc.)

The magnetic ring was composed of 4 coaxial rings which were magnetized in the radial direction. Initially the magnet was set 11mm from the superconductor and the superconductor was cooled to the superconducting state by liquid nitrogen. The temperature of the liquid nitrogen was 77K, and the Y-Ba-Cu-O superconductor reached the superconducting state under 92K. After field cooling, the magnetic ring was moved gradually to 2mm from the surface of the superconductor, then moved gradually to 11mm away and moved back gradually to 2mm away.

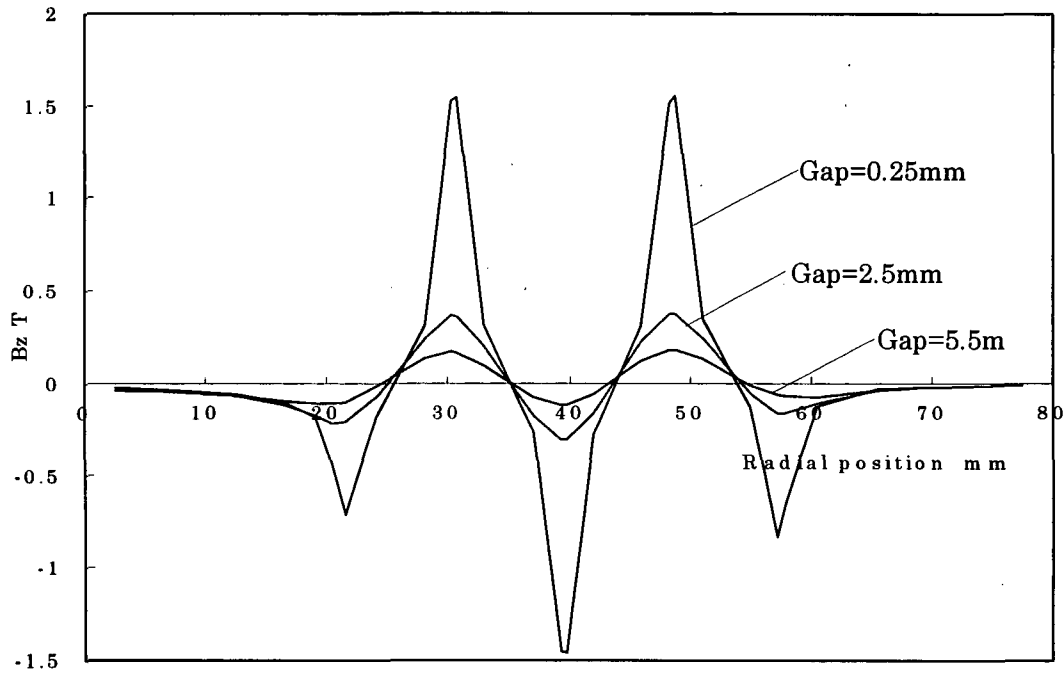


Figure 11. B_z of the magnetic field

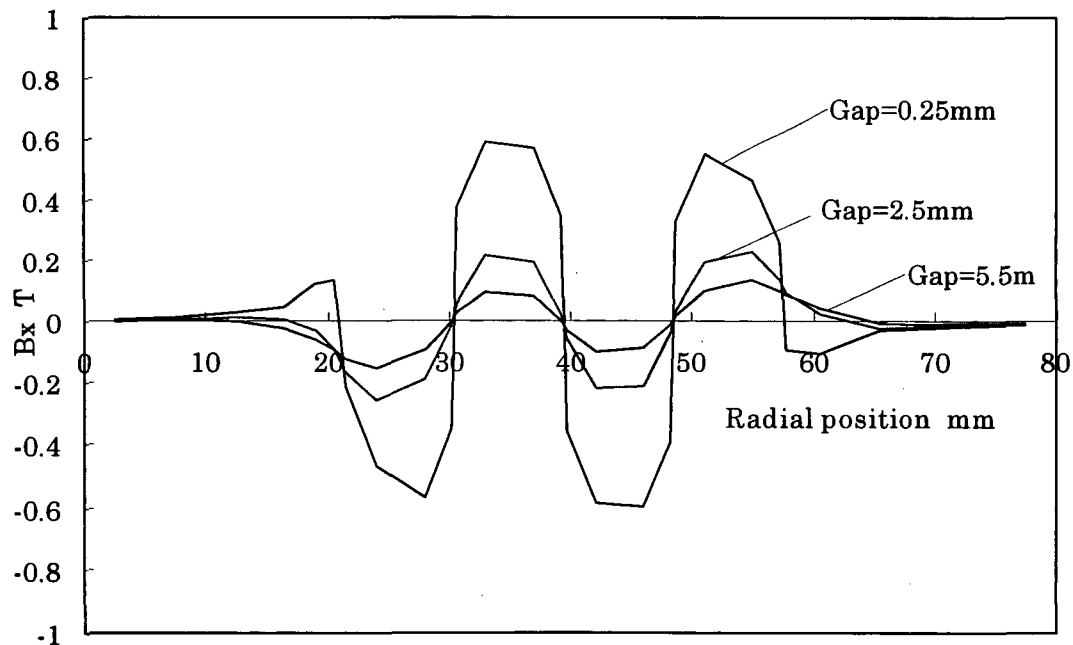


Figure 12. B_x of the magnetic field

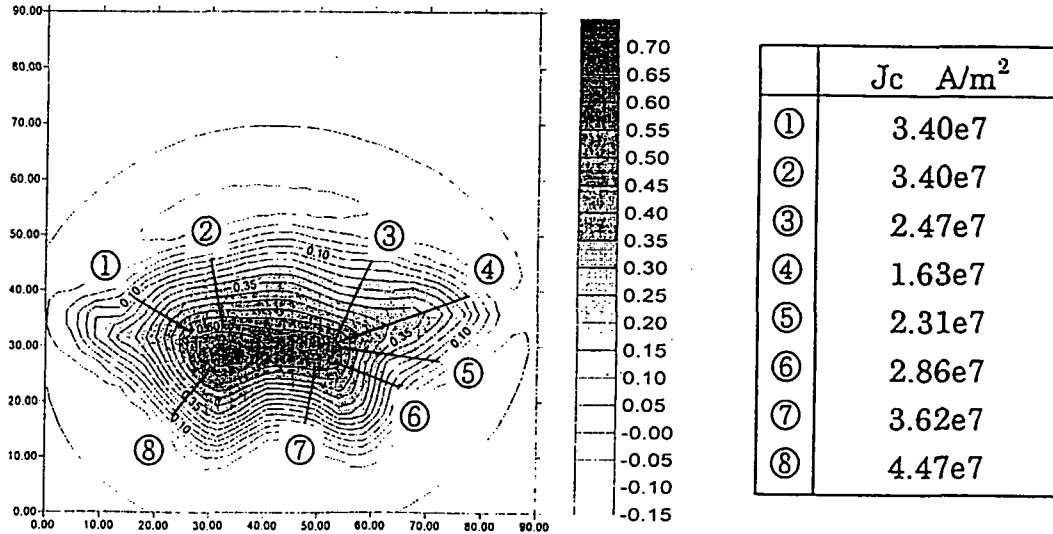


Figure 13. J_c of superconductor(Nippon Steel Corp.)

Now, we should be better to refer the contribution of $m_x \frac{\partial B_z}{\partial x} + m_y \frac{\partial B_z}{\partial y}$ in F_z calculation.

In axisymmetric case, we need not consider $m_y \frac{\partial B_z}{\partial y}$ but only $m_x \frac{\partial B_z}{\partial x}$. In Figure 12, $\frac{\partial B_z}{\partial x}$

alternates in radial direction, and this causes the contribution of $m_x \frac{\partial B_z}{\partial x}$ to F_z becomes negligible as shown in Figure 14.

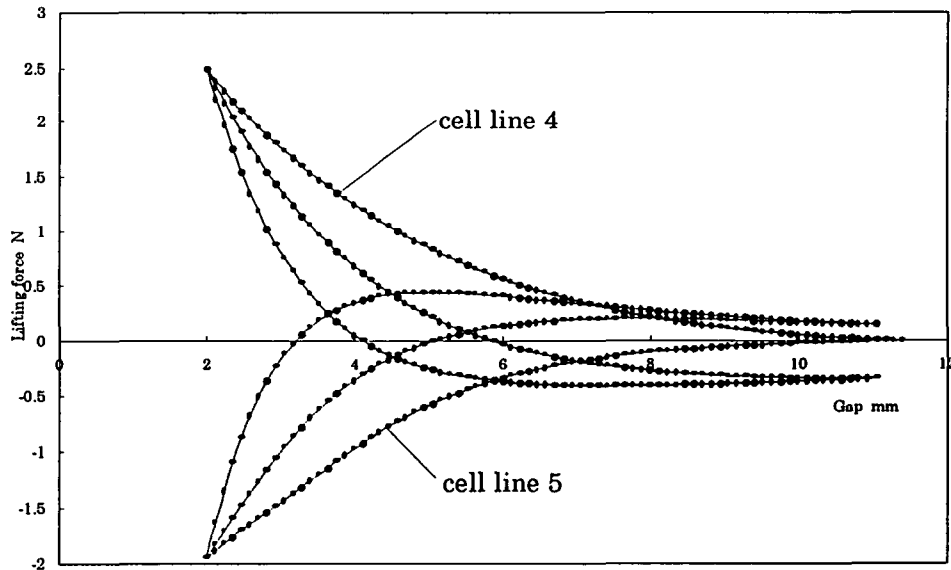


Figure 14. Levitation force curves of 2 cells at different radial position

Examples of experimental and calculated results are shown in Fig.15. The experiment was conducted as follows. J_c of the single crystal superconductor was estimated as about 2.6×10^7 from Figure 13.

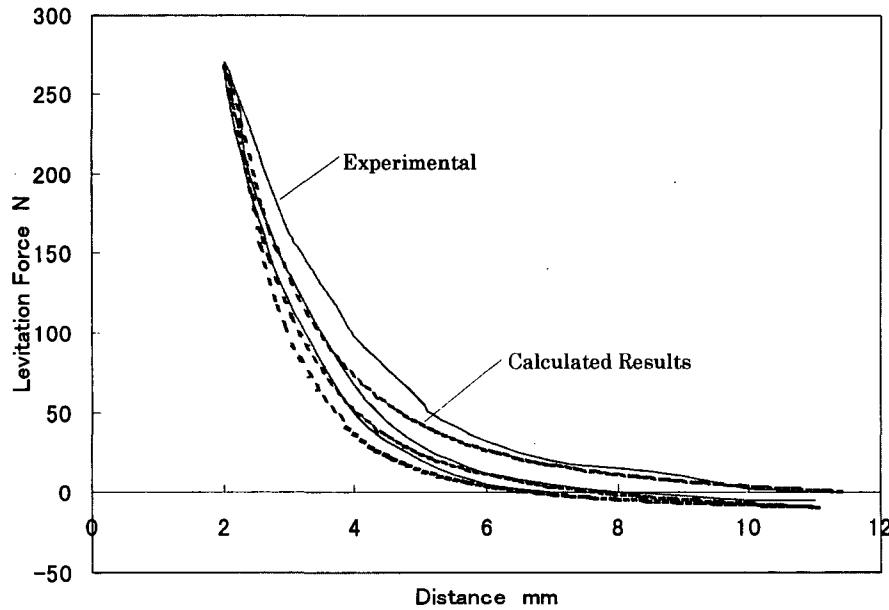


Figure 15. Experimental and Calculated Results

Fig.16 is another test rig using $\phi 65 \times \phi 40 \times t20$ MPMG (Melt-Powder-Melt-Growth) superconductor. In the experiment, magnet and superconductor was set contact in field cooling, and then the process of removing and approaching of the magnet to the superconductor was repeated. Fig. 17 is the comparison between the experimental and calculated result. Looking at Fig.15 and Fig.17, it can be understood that the calculated result shows good agreement with the experimental result.

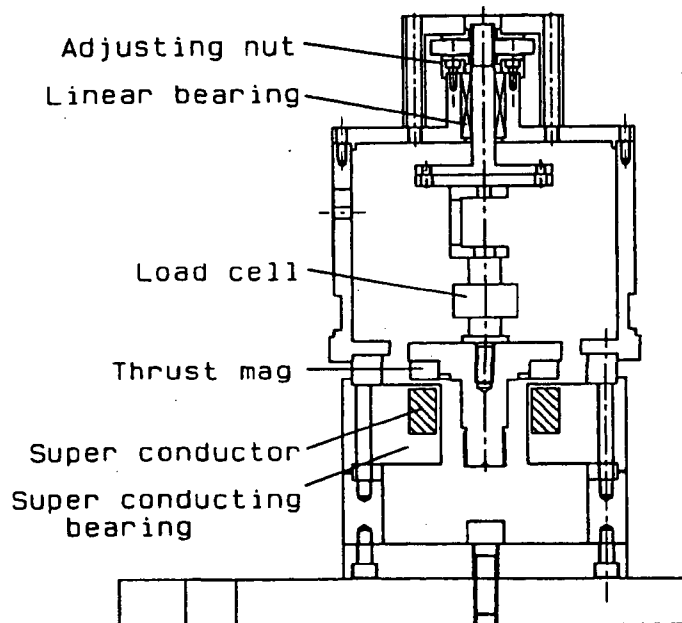


Figure 16 Test rig2

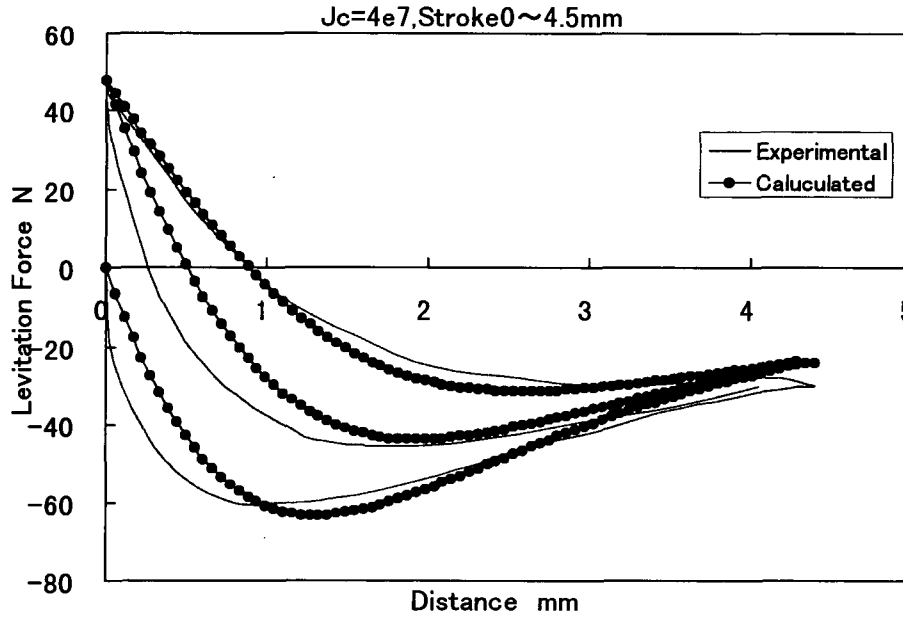


Figure 17. Experimental and calculated result of levitation test

ANALYSIS OF LEVITATION CHARACTERISTICS

The effect of field cooling position is shown in Fig.14 when H_u, H_L and J_c are constant. Maximum repulsive force becomes large as the field cooling distance becomes large. The effect of superconductor thickness is shown in Fig.15 when H_u, H_L, H_0 and J_c are constant. Superconductor thickness does not affect levitation force when it becomes too large. Fig.16 shows the effect of J_c on maximum levitation force when H_u, H_L and H_0 are constant.

From Fig 11, we can understand that if H_u, H_L and H_0 are limited, maximum levitation force becomes saturated even if we achieve very high J_c . Fig 12 shows the effect of the single crystal superconductor size. The effect of the single crystal size is very large.

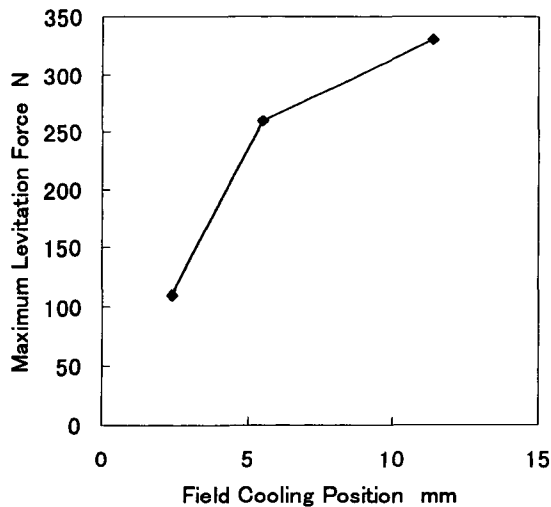


Figure 18. Effect of Field Cooling Position

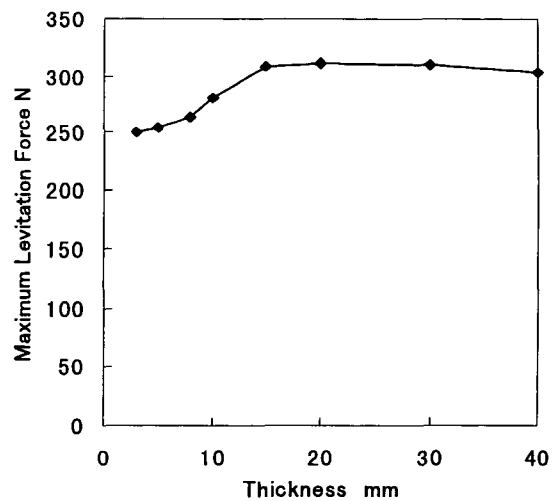


Figure 19. Effect of Thickness of Superconductor

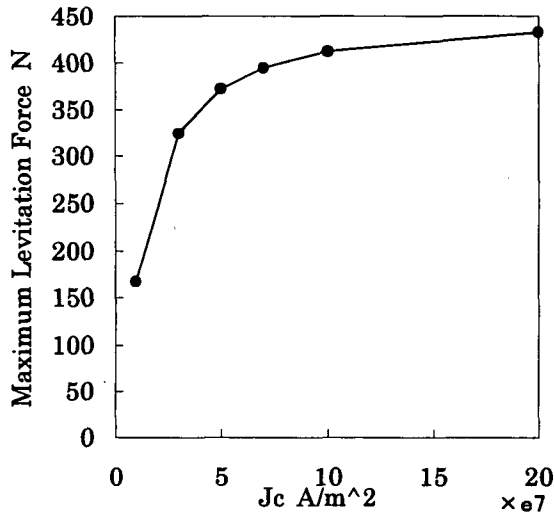


Figure 20. Effect of Jc

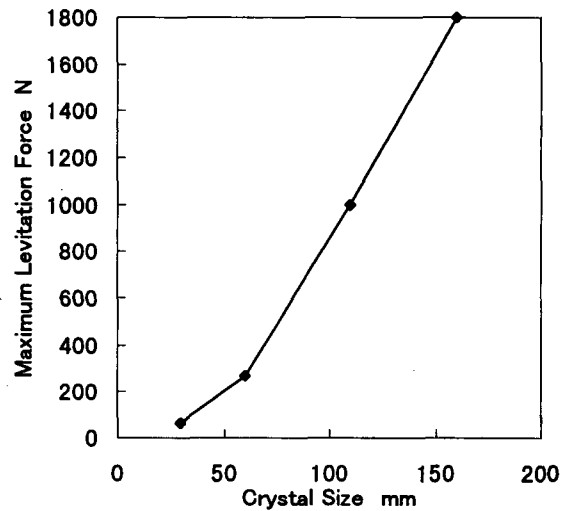


Figure 21. Effect of Crystal Size

CONCLUSION

The following conclusions were obtained.

- (1) The magnetization generated in a superconductor in a complicated magnetic field can be calculated by meshing the superconductor, and applying both electromagnetic FEM and the 2 dimensional Bean model to the cells.
- (2) Magnetization hysteresis by the 2 dimensional Bean model is grouped into 31 cases according to the parameters of a, b, J_c, H_0 and ΔH under the restriction that $2a > b > a$ and subroutines should be made to calculate them in order to enable the calculation of any size and shape of superconductor.
- (3) In order to calculate real magnetization of meshed cells, a correcting calculation should be carried out.
- (4) Levitation force hysteresis can be obtained by calculating magnetization hysteresis and levitation force hysteresis of meshed cells and summing them up for all cells.
- (5) The contribution of $m_x \frac{\partial B_z}{\partial x}$ to F_z is negligible in ordinary cases.
- (6) Maximum repulsive force increases as field cooling distance becomes large.
- (7) Increasing superconductor thickness does not lead to increased levitation force after exceeding some limiting value.
- (8) In spite of increasing J_c , there is a limit to increasing levitation force if H_u, H_L and H_0 do not change.
- (9) Increasing the single crystal size brings about a very large increase in levitation force.

ACKNOWLEDGEMENTS

The authors are pleased to acknowledge that this work was carried out under the contract of the project 「The Research and Development of Electric Energy Storage by Flywheel using High

Temperature Superconductor] by New Energy and Industrial Technology Development Organization (NEDO).

REFERENCES

1. Morita, M. et al. 1994. "Processing and properties of QMG materials," *Physica C* (235-240):209-212
2. Murakami, M. et al. 1990. "Large levitation force due to flux pinning YBaCuO superconductors fabricated by Melt-Powder-Melt-Growth Process," *Jpn.J.Appl.Phys.*29, L1991
3. Moon, F.C., Weng, K.C. and Chang, P.Z. 1990. "Dynamic magnetic forces in superconducting ceramics," *Appl.Phys.*L56:397
4. Takahata, R., Ueyama, H. and Yotsuya, T. 1992. "Load carrying capacity of superconducting magnetic bearings," *Electromagnetic Forces and Applications*, Elsevier .1:347
5. Fukuyama, H. et al. 1992. "Superconducting Magnetic Bearings Using MPMG-YBaCuO," *Adv. in Superconductivity IV*:1093-1096
6. Ogiwara, H., Azukizawa, T. and Morishita, M. 1993. "A Novel Use of Superconducting Oxides in a Non-contact Carrier for VLSI Plants," *Appl. Superconductivity 1* (3-6):1185-1192
7. Higasa, H., Ishikawa, F. et al. 1994. "Experiment of a 100Wh-Class Power Storage System using High-Tc Superconducting Magnetic Bearing," *Adv. in Superconductivity VI*:1249-1252
8. Bornemann, H.J. et al. 1994. "A FLYWHEEL FOR ENERGY STORAGE WITH FRICTIONLESS HIGH TEMPERATURE SUPERCONDUCTOR BEARINGS," 4th Int. Sym. On Magnetic Bearings, Aug.
9. Albanese, R. et al. 1994. "DESIGN, CONSTRUCTION AND TESTING OF A KINETIC ENERGY STORAGE DEVICE WITH HIGH-Tc SUPERCONDUCTIVE SUSPENSION," 4th Int. Symp. on Magnetic Bearings, Aug.
10. Chu, W. et al. 1995. "HYBRID SUPERCONDUCTING MAGNETIC BEARINGS FOR FLYWHEEL ENERGY STORAGE SYSTEMS," Int. Workshop on Superconductivity Co-Sponsored by ISTE and MRS, June
11. Chang, P.Z. 1991. Ph.D. Thesis. Cornell Univ.
12. Sugiura, T., Hashizume, H. and Miya, K. 1991. "Numerical electromagnetic field analysis of type-II superconductors," *Int. J. Appl. Electromagn. Mater.* 2:183
13. Bean, C.P. 1962. "Magnetization of hard superconductors," *Phys. Rev. Lett.*, 8:250
14. Hashizume, H. et al. 1991. "Numerical analysis of coupling loss in superconductor," *Cryogenics*, 31:601
15. Uesaka, M., Yoshida, Y., Takeda, N. and Miya, K. 1993. "Experimental and numerical analysis of three dimensional high Tc superconducting systems," *Int. J. Appl. Electromagn. Mater.*, 4:13
16. Tsuchimoto, M., Takeuchi, H. and Honma, T. 1994. " Numerical Analysis of Levitation Force on a High Tc Superconductor for Magnetic Field Configuration," *T. IEE Jpn.* 114-D, 7/8:741